Extraction of the Landau-Migdal Parameter from the Gamow-Teller Giant Resonance in ^{132}Sn

J. Yasuda *et al.*

Extraction of the Landau-Migdal parameter from the Gamow-Teller Giant Resonance in ^{132}Sn

J. Yasuda,[1,2] M. Sasano,[2] R. G. T. Zegers,[3,4,5] H. Baba,[2] D. Bazin,[3] W. Chao,[2] M. Dozono,[2] N. Fukuda,[2]
N. Inabe,[2] T. Isobe,[2] G. Jhang,[2,3] D. Kameda,[2] M. Kaneko,[6,2] K. Kisamori,[2,7] M. Kobayashi,[7] N. Kobayashi,[8]
T. Kobayashi,[2,9] S. Koyama,[2,8] Y. Kondo,[10,2] A. J. Krasznahorkay,[11] T. Kubo,[2] Y. Kubota,[2,7]
M. Kurata-Nishimura,[2] C. S. Lee,[2,7] J. W. Lee,[12] Y. Matsuda,[13] E. Milman,[2,14] S. Michimasa,[7] T. Motobayashi,[2]
D. Muecher,[2,15,16] T. Murakami,[6] T. Nakamura,[10,2] N. Nakatsuka,[2,6] S. Ota,[7] H. Otsu,[2] V. Panin,[2]
W. Powell,[2] S. Reichert,[2,15] S. Sakaguchi,[1,2] H. Sakai,[2] M. Sako,[2] H. Sato,[2] Y. Shimizu,[2] M. Shikata,[10,2]
S. Shimoura,[7] L. Stuhl,[2] T. Sumikama,[9,2] H. Suzuki,[2] S. Tangwancharoen,[2] M. Takaki,[7] H. Takeda,[2] T. Tako,[9]
Y. Togano,[10,2,17] H. Tokieda,[7] J. Tsubota,[10,2] T. Uesaka,[2] T. Wakasa,[1] K. Yako,[7] K. Yoneda,[2] and J. Zenihiro[2]

[1]*Department of Physics, Kyushu University, Nishi, Fukuoka 819-0395, Japan*
[2]*RIKEN Nishina Center, Hirosawa 2-1, Wako, Saitama 351-0198, Japan*
[3]*National Superconducting Cyclotron Laboratory, Michigan State University, East Lansing, Michigan 48824, USA*
[4]*Joint Institute for Nuclear Astrophysics, Michigan State University, East Lansing, Michigan 48824, USA*
[5]*Department of Physics and Astronomy, Michigan State University, East Lansing, Michigan 48824, USA*
[6]*Department of Physics, Kyoto University, Kyoto 606-8502, Japan*
[7]*Center for Nuclear Study, University of Tokyo, Bunkyo, Tokyo 113-0033, Japan*
[8]*Department of Physics, University of Tokyo, Tokyo, 113-0033, Japan*
[9]*Department of Physics, Tohoku University, Miyagi 980-8578, Japan*
[10]*Department of Physics, Tokyo Institute of Technology,*
2-12-1 O-Okayama, Meguro, Tokyo 152-8551, Japan
[11]*ATOMKI, Institute for Nuclear Research, Hungarian Academy of Sciences, Debrecen, Hungary*
[12]*Department of Physics, Korea University, Seoul 02841, Republic of Korea*
[13]*Department of Physics, Faculty of Science and Engineering,*
Konan University, 8-9-1 Higashinada, Kobe, Hyogo, 658-8501, Japan
[14]*Department of Physics, Kyungpook National University, Daegu 702-701, Korea*
[15]*Technical University of Munich, Munich, Germany*
[16]*Department of Physics, University of Guelph, Ontario N1G 2W1, Canada*
[17]*Department of Physics, Rikkyo University, Tokyo 171-8501, Japan*
(Dated: August 21, 2018)

The key parameter to discuss the possibility of the pion condensation in nuclear matter, i.e. the so-called Landau-Migdal parameter g', was extracted by measuring the double-differential cross sections for the (p, n) reaction at 216 MeV/u on a neutron-rich doubly magic unstable nucleus, ^{132}Sn with the quality comparable to data taken with stable nuclei. The extracted strengths for Gamow-Teller transitions from ^{132}Sn leading to ^{132}Sb exhibit the GT giant resonance (GTR) at the excitation energy of 16.3 ± 0.4(stat.) ± 0.4(syst.) MeV with the width of $\Gamma = 4.7 \pm 0.8$ MeV. The integrated GT strength up to $E_x = 25$ MeV is $S_{\mathrm{GT}}^- = 53 \pm 5$(stat.) $^{+11}_{-10}$(syst.), corresponding to 56% of Ikeda's sum rule of $3(N - Z) = 96$. The present result accurately constrains the Landau-Migdal parameter as $g' = 0.68 \pm 0.07$, thanks to the high sensitivity of the GTR energy to g'. In combination with previous studies on the GTR for ^{90}Zr and ^{208}Pb, the result of this work shows the constancy of this parameter in the nuclear chart region with $(N - Z)/A = 0.11$ to 0.24 and $A = 90$ to 208.

A giant resonance (GR) is a collective oscillation mode of an atomic nucleus and also a feature of quantum many-body systems [1]. The Gamow-Teller (GT) giant resonance (GTR) is the oscillation in the spin and isospin degrees of freedom, without changes in the spatial wave function [2–8]. The GTR has attracted strong interests [7, 8] as an experimental method for calibrating the interaction causing the pion condensation predicted by Migdal, a candidate of phase transitions in nuclear matter such as the interior of a neutron star [9]. In addition, the GT excitations are closely related to weak processes of astrophysical and fundamental interests [10, 11].

Occurrence of the pion condensation is dictated by the spin-isospin interaction in the nuclear medium, whose be-

havior is very characteristic in terms of the interaction ranges: The spin-isospin interaction, through its long-range and attractive component, facilitates pion condensation. However, through its short-range and repulsive component, it hampers the onset of this phase transition. Theoretically, the long-range and attractive component comes from the one pion-exchange potential and can be described relatively well. In contrast, the short-range and repulsive component contains the effects of complex phenomena occurring in that range, which are central to better understanding nuclear many-body theories [12].

Instead of solving complex many-body problems, Migdal represented the strength of the short-range component by a simple constant called the Landau-Migdal

(LM) parameter g' [9, 13]. Despite of its simplicity, g' well characterizes the phase diagram of nuclear matter. Pion condensation occurs if g' is smaller than a certain critical value (g'_c), which can be derived relatively easily as $g'_c = 0.3$ to 0.5 for isospin-symmetric nuclear matter at nuclear saturation density [13].

In exchange for simplicity, however, theoretical predictions of g', which contains all the complexity of the short-range component, are very challenging and the value must be evaluated experimentally. Essentially, the collectivity of the GTR comes only from the short-range component of the spin-isospin interaction. As a result, the GTR energy increases with the increase of g', thereby serving as a sensitive probe of g'.

In this Letter, we report data on the GTR in ^{132}Sn by using the charge-exchange (CE) (p, n) reaction with an RI beam to provide a new and rare calibration point for g' in the wide nuclear chart including unstable nuclei. The measurement demonstrates that accurate information about isovector spin-flip giant resonances can be obtained for unstable nuclei by using this probe, including key cases such as doubly magic ^{132}Sn.

At present, the most reliable calibration on g' is given by the GTR data on a doubly magic stable nucleus ^{208}Pb [14]. For a given change in g', the GTR-energy shift is proportional to the isospin asymmetry $(N - Z)/A$ [15]. Because of its large isospin asymmetry of $(N - Z)/A = 0.21$, the GTR in ^{208}Pb provides a good way to calibrate g'. In Ref. [14], g' was adjusted as $g' = 0.64$ to reproduce the measured GT strength distribution for ^{208}Pb over a wide excitation energy region including the GTR with the random phase approximation (RPA).

This method is considered to be reliable but the application is limited to doubly magic nuclei because of the use of the RPA. With the same method, the GTR of another doubly magic nucleus ^{90}Zr is also examined, giving a slightly smaller but consistent g' value, 0.6 ± 0.1 [16]. However, the sensitivity of the GTR in ^{90}Zr is weaker by a factor of two because of the smaller isospin asymmetry $(N - Z)/A = 0.11$. There have been also discussions based on the energy-weighted sum rule, which surprisingly show a large variation of g': $g' = 0.490$ (^{48}Ca), 0.595 (^{90}Zr), and 0.722 (^{208}Pb) [15].

Consequently, it is an open question whether the value of g' extracted from ^{208}Pb is valid across the chart of nuclei and whether it could go below g'_c. A major uncertainty in the extraction of g' comes from the perturbation of the GT strength distribution by single-particle structure effects [17]. In combination with the fact that the single-particle structure effects are stronger in lighter nuclei, the lower sensitivity makes it more difficult to extract g' from the light nuclei compared to heavy closed-shell systems [17]. The study of ^{132}Sn provides an important calibration point for g'. Like ^{208}Pb it is doubly magic and it has an even higher isospin asymmetry of

0.24.

Experimentally, the CE (p, n) reaction at intermediate energies ($\gtrsim 100$ MeV/u) is a powerful tool to study the GT transition thanks to the proportionality relation between the zero angular-momentum transfer ($\Delta L = 0$) cross section at a foward angle [$\sigma_{\Delta L = 0}(q, \omega)$] and the corresponding GT strength $B(\mathrm{GT})$ [18],

$$\sigma_{\Delta L=0}(q, \omega) = \hat{\sigma}_{\mathrm{GT}} F(q, \omega) B(\mathrm{GT}). \tag{1}$$

Here, $\hat{\sigma}_{\mathrm{GT}}$ is the GT unit cross section and $F(q, \omega)$ represents the dependence of $\sigma_{\Delta L=0}(0°)$ on the momentum (q) and energy (ω) transfers. $F(q, \omega)$ takes the value of unity at the limit of $q = 0$ and gradually changes as a function of q. By using this proportionality, one can extract the GT transition strengths over a wide excitation-energy region including the region of the GTR.

For studying the CE reactions on ^{132}Sn, we employed a technique for measuring (p, n) reactions in inverse kinematics recently developed [19, 20]. In this technique one can obtain excitation-energy spectra over a wide energy region with good statistics by using the missing-mass spectroscopy with a thick target. In this work, the technique was further developed such that many relevant decay channels after the CE reaction can be measured in a single magnetic rigidity setting with the large acceptance spectrometer SAMURAI [21].

The experiment was performed at Radioactive Isotope Beam Factory (RIBF) in RIKEN. A cocktail beam containing ^{132}Sn was produced by projectile fragmentation of a ^{238}U primary beam at 345 MeV/u colliding with a 4-mm thick ^{9}Be target. The total intensity of the beam
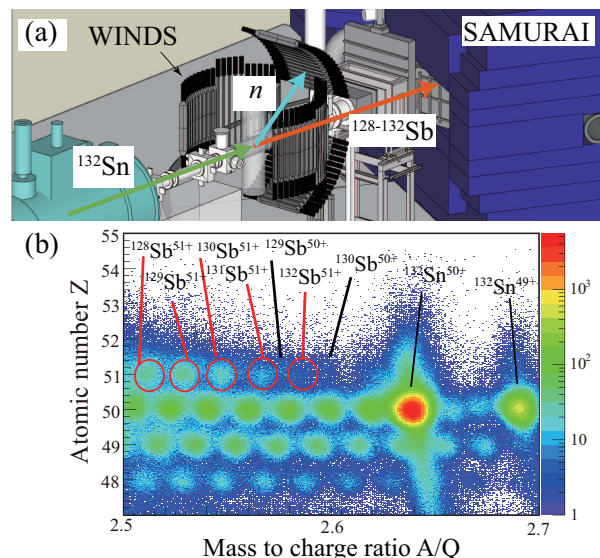

FIG. 1. A schematic view of the experimental setup around the hydrogen target (a). A PID plot produced with the SAMURAI spectrometer associated with the ^{132}Sn incoming beam (b).

was 1.4×10^4 pps and the purity of ^{132}Sn was about 45%. In the present data analysis, events associated with ^{132}Sn incoming beam particles were selected. The secondary beam was transported onto an 11-mm thick liquid hydrogen target. The target had an average thickness of 70.9 mg/cm^3 and was contained by 19-μm thick Havar foils. The beam energy at the target midpoint was 216 MeV/u.

Figure 1(a) shows the setup around the target. Recoil neutrons from the (p,n) reaction were detected using the WINDS neutron detector [22, 23]. The scattering angles ($\theta_{\rm lab}$) from 20° to 122° in the laboratory frame were covered. The neutron energy (E_n) was determined by measuring the neutron time of flight (TOF). The light-output threshold was set to 40 keV$_{ee}$ (electron equivalent). Neutron-detection efficiencies, ranging from 70% at $E_n = 0.6$ MeV to 50% at $E_n = 4$ MeV, were calculated using the simulation code GEANT4 [24]. The validity of the simulations was confirmed by comparing with measured efficiencies using a ^{252}Cf fission source.

For tagging the CE-reaction channel, the residues were analyzed by the SAMURAI spectrometer [21]. The magnetic field of the spectrometer was set to 2.54 T. The particle identification (PID) was performed through the TOF-$B\rho$-ΔE method (see Ref. [23] for details). Using the PID plot shown in Fig. 1(b), events associated with $^{128-132}$Sb isotopes were selected, covering the decay channels by $1n$–$4n$ emissions after the (p,n) reaction.

The excitation energy (E_x) and center-of-mass scattering angle ($\theta_{\rm c.m.}$) were reconstructed from the measured E_n and $\theta_{\rm lab}$ values. The excitation-energy resolution ΔE_x varies from 1.0 MeV to 2.5 MeV (FWHM) with increasing $\theta_{\rm c.m.}$ from 2° to 10°. Background events due to reactions on the target-cell windows and beam detectors were evaluated from measurements with an empty target cell. A second source of background was due to neutrons hitting WINDS indirectly after scattering off surrounding objects [19, 20]. This background was estimated and subtracted in the same manner as described in Refs. [19, 20] by using ^{132}Sb $\to$ ^{127}Sb $+ 5n$ events, because ^{127}Sb cannot be created in the decay of ^{132}Sb excited to energies under consideration.

The left panel of Fig. 2 shows the obtained double-differential cross sections for the ^{132}Sn(p,n) reaction at 216 MeV/u. The data points represent the sums of the events associated with the detection of $^{128-132}$Sb in the SAMURAI spectrometer. It should be noted that the decay branches associated with one-proton emission to ^{131}Sn were found to be small: $7 \pm 4\%$ for $E_x = 12$–20 MeV. In this analysis, these small contributions are neglected. Since the excitation-energy resolution deteriorated with increasing scattering angle, for the purpose of multi-pole decomposition analysis (MDA) described below, the spectra were smeared with Gaussians to achieve a resolution of 2.5 MeV (FWHM) at each angle, as done

in Refs. [19, 20].

To apply the proportionality, the $\Delta L = 0$ contributions must be isolated from contributions with $\Delta L > 0$. This was done by performing an MDA [8]. The experimental angular distribution of the differential cross section for each excitation energy bin was fitted with a linear combination of theoretical angular distributions associated with $\Delta L = 0$, 1, and 2, as shown in the right panels of Fig. 2. The theoretical angular distributions were obtained by employing the DWIA formalism described in Ref. [25] with the use of the computer code CRDW, in conjunction with the effective interaction from Ref. [26] and optical potentials from Refs. [27–29]. Transition densities based on the RPA formalism described in Ref. [14] were used, as described below. The MDA result in Fig. 2 shows that the yield at forward angles is predominantly due to GT ($\Delta L = 0$) transitions for excitation energies up to 20 MeV. Above that, there are contributions from dipole $\Delta L = 1$ and quadrupole $\Delta L = 2$ excitations.

The extracted $B(\rm GT)$ distribution is shown in Fig. 3(a). The value of $\hat{\sigma}_{\rm GT}$ was set to 2.7 ± 0.5 mb/sr based on the mass-number dependence studied at 200 MeV [30]. The kinematic factor F was obtained through the above mentioned DWIA calculations. The spectrum clearly exhibits a strong GTR peak at 16 MeV with a shoulder structure around 12 MeV. The spectrum includes a contribution from the isobaric analog state (IAS) of the ^{132}Sn ground state in ^{132}Sb. The IAS peak position was estimated to be $E_{\rm IAS} = 15.6 \pm 0.2$ MeV by using the phenomenological function [31]. The IAS
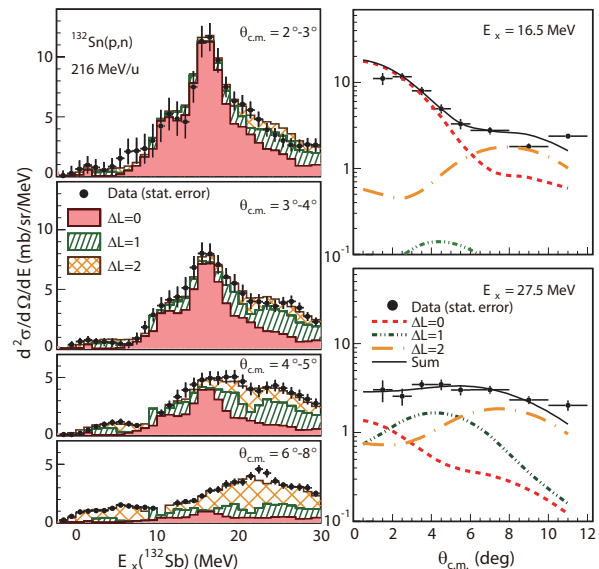

FIG. 2. (Left) double-differential cross sections and the results of the MDA of the ^{132}Sn(p,n) data. The error bars denote the statistical uncertainty only. (Right) angular distributions of the different cross section at $E_x = 16.5$ and 27.5 MeV in comparison with the fitting curves in the MDA.

contribution corresponding to the GT strength unit was estimated as 1.8 ± 0.2 from the Fermi sum rule strength of $N - Z = 32$. Here we took into account the ratio of the Fermi unit cross section, $\hat{\sigma}_F = 0.15$ mb/sr [30], to the $\hat{\sigma}_{GT}$ value, 2.7 mb/sr. The contribution of the unobserved one-proton emission branch to the IAS, ~ 0.18 in the GT strength unit, was neglected. The shaded bands represent the systematic uncertainties, which are dominated by the uncertainties in the background subtraction ($< 15\%$), the efficiency correction ($< 15\%$), and the input parameters of the DWIA calculation ($< 3\%$). The total strength up to $E_x = 25$ MeV is $S_{GT}^- = 53 \pm 5(\text{stat.})_{-10}^{+11}(\text{syst.})$, where the IAS contribution has been already subtracted and the uncertainty in $\hat{\sigma}_{GT}$ is not included. The systematic uncertainty is mainly due to the uncertainties in the background subtraction and the efficiency correction. The present total strength corresponds to $56 \pm 5(\text{stat.})_{-10}^{+11}(\text{syst.})\%$ of the non-energy-weighted sum-rule value (so-called Ikeda's sum rule) of $3(N - Z) = 96$, which is consistent with the systematics in stable nuclei [6].

The GTR energy was obtained to be $E_{GT} = 16.3 \pm 0.4(\text{stat.}) \pm 0.4(\text{syst.})$ MeV, where the first and second uncertainties are the statistical and systematic uncertainties, respectively. The main sources of the systematic uncertainty come from the uncertainty of the beam energy (~ 0.24 MeV) and the fitting procedure (~ 0.2 MeV). Figure 3(b) shows the fitting results used for determining the centroid value. Here, three components, the GTR, the lower-lying shoulder, and the IAS are considered. For the GTR and shoulder components, in order to take into account the experimental energy resolution of $\Delta E_x = 2.5$ MeV, we used a Voigt function. A Gaussian function was used for the IAS contribution. The width of the GTR was estimated to be $\Gamma = 4.7 \pm 0.8$ MeV, which is close to those of the stable Sn isotopes [32]. We note that the extraction of the resonance parameters in this work has similar quality to data from measurements with stable beams in forward kinematics [14, 16, 32, 33], which has never been realized in past studies of GRs with RI beams [34, 35] in terms of the uncertainties of the derived resonance parameters.

The LM parameter, g', was deduced by comparing the data with theoretical strength distributions assuming different g' values, as shown with curves in Fig. 3(a). Herein, we followed the exactly same method as in Refs. [14, 16]: The continuum RPA [8] is used for the description of the response properties, and the single-particle energy levels taken from experimental data for the static structure properties. The $\pi + \rho + g'$ model interaction [8] was employed as an effective interaction. In the present model, the LM contact interaction includes the coupling to the Δ particle calibrated in Ref. [8]. Single-particle wave functions were generated by a Woods-Saxon (WS) potential with $r_0 = 1.27$ fm, $a_0 = 0.67$ fm, and $V_{SO} = 7.5$ MeV [31]. The depths of the WS poten-
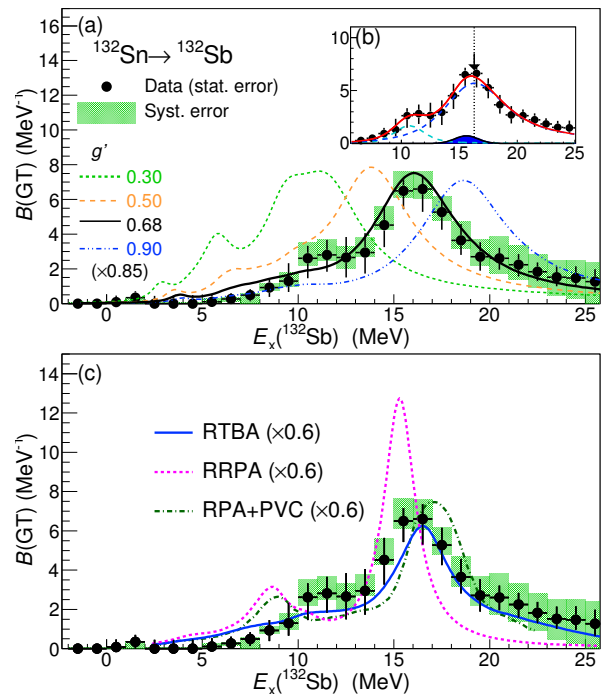

FIG. 3. Extracted GT strength distribution in ^{132}Sb and the comparison with the RPA calculation with the $\pi + \rho + g'$ interaction model with different g' values of 0.30, 0.50, 0.68, and 0.90 (a). (b) shows the result of fitting procedure described in the text. The shaded area indicates the contribution from the IAS. (c) shows the same as (a) but for the comparison with self-consistent nuclear-model calculations.

tials for neutrons and protons were adjusted to reproduce the separation energies of $0h_{11/2}$ and $0g_{9/2}$ orbits [36], respectively. Here, a factor of 0.85 is multiplied to the calculated spectrum for comparison with data. The calculated GTR energy changes as a function of g'. The calculations with $g' = g'_c$ at saturation density, 0.3–0.5, are rejected by this comparison. Rather it clearly shows that g' is larger than g'_c. The g' value best reproducing the data is $g' = 0.68 \pm 0.07$. The overall structure of the calculated spectrum best fits with the data at this g' value. The uncertainty is due to the experimental peak energy (~ 0.05) and the input for the theoretical calculation (~ 0.05). The theoretical uncertainty was estimated by changing the WS potentials for the single particle wave functions. The present g' value is close to the values of ^{90}Zr (0.6 ± 0.1) [16] and ^{208}Pb (0.64) [14].

In the above approach, the static structure of nuclei is treated separately from the response and, as a result, there may be some fluctuation in the extracted g' values depending on individual nuclei. A way to avoid such problems is to use self-consistent nuclear models [17, 37–39], in which the static structure and response of various nuclei are treated within the same framework. Shown in Fig. 3(c) are self-consistent

model calculations performed using the relativistic time-blocking approximation (RTBA) [38, 40], relativistic RPA (RRPA) [39, 41], and RPA with particle-vibration coupling (RPA+PVC) [37], which have been smeared to take into account the experimental resolution. The RRPA does not include higher-order effects such as PVC, while the others do. Therefore the RRPA has a narrower GTGR peak. The RTBA calculation uses the NL3 interaction model, whose g' is fixed at 0.6 to reproduce the GTR energy in ^{208}Pb [42]. In the RRPA and RPA+PVC calculations, there is no parameter directly corresponding to g' and the model parameters are fixed using the ground-state properties of heavy nuclei. All of these calculations reproduce the GT energy in ^{132}Sn with a difference better than 1 MeV, as shown in Fig. 3(c). We note that these calculations also reproduced the GTR energy in ^{90}Zr [39, 43, 44]. The 1-MeV shift in the GTR energy corresponds to the shift in g', $\delta g' \sim 0.08$, which is much smaller than the variation reported in Ref. [15]. This indicates g' or the set of the model parameters equivalent to g' in these models is almost constant, at least within the region between ^{90}Zr, ^{132}Sn, and ^{208}Pb.

The shoulder around 11 MeV is reproduced in the RTBA and the continuum RPA calculations. The RPA+PVC and RRPA calculations exhibit a bump about 3 MeV lower than in the data. In the continuum RPA, the shoulder is primarily due to contributions from one-particle one-hole excitations in the g orbits. In the RRPA and RPA+PVC calculations, there is a relatively strong contribution from d orbits. In the RTBA calculation, there are no predominant configurations and the coherence between different configurations is not obvious [45]. Clearly, the low-energy weakly collective part of the GT distribution is very sensitive to details of the shell structure in the models. We note that the shell-model calculation in Ref. [38] reproduces the GTR equally well as the self-consistent model calculations, which will help the understanding of the shell structures.

In summary, the double-differential cross sections for the ^{132}Sn(p,n) reaction at 216 MeV/u were measured. In the experiment, we demonstrated that information about the strength distribution of isovector spin-flip giant resonances can be obtained from (p,n) experiments in inverse kinematics with RI beams, being similar in quality to that obtained from experiments with stable target in forward kinematics. The GTR was observed at $E_x = 16.3 \pm 0.4$(stat.) ± 0.4(syst.) MeV with the width of $\Gamma = 4.7 \pm 0.8$ MeV. The integrated $B(GT)$ up to $E_x = 25$ MeV is $S_{GT}^{-} = 53 \pm 5$(stat.) $^{+11}_{-10}$(syst.), corresponding to 56% of Ikeda's sum-rule of $3(N - Z) = 96$. The present data constrains the LM parameter of ^{132}Sn as $g' = 0.68 \pm 0.07$, which is close to the calibration value 0.64 for the ^{208}Pb case with the same theoretical framework. Three different self-consistent nuclear models calibrated by the ^{208}Pb GTR data all reproduce the GTR energy of ^{132}Sn within the difference of 1 MeV cor-

responding to a small shift of $\delta g' \sim 0.08$. Consequently, g' appears to be almost constant in the region of nuclear chart situated between ^{90}Zr, ^{132}Sn, and ^{208}Pb. Assuming that g' is a function of the isospin asymmetry $(N - Z)/A$ and the mass number A, this also means that g' is constant in the range from $(N - Z)/A = 0.11 - 0.24$ and from $A = 90$ to 208. If the present g' value is kept to be constant up to the extreme of $(N - Z)/A = 1$, it is considered that the pion condensation should occur around two times of normal nuclear density, which can be realized in a neutron star with a mass of 1.4 times that of the sun [8]. For the future, it is essential to investigate if such a constant behavior of g' is valid for even broader isospin range to understand the possibility of the pion condensation fully. For that, we plan to apply the current method to a longer Sn isotopic chain including proton-rich isotopes near ^{100}Sn, where $(N - Z)/A = 0$, as well as neutron-rich nuclei beyond the present limit $(N - Z)/A = 0.24$.

[1] M. N. Harakeh and A. van der Woude, *Giant Resonances: Fundamental high-Frequency Modes of Nuclear Excitations* (Oxford University Press, New York, 2002).

[2] K. Ikeda, S. Fujii, and J. I. Fujita, Phys. Lett. **3**, 271 (1963).

[3] R. R. Doering, Aaron Galonsky, D. M. Patterson, and G. F. Bertsch, Phys. Rev. Lett. **35**, 1691 (1975).

[4] D. E. Bainum, J. Rapaport, C. D. Goodman, D. J. Horen, C. C. Foster, M. B. Greenfield, and C. A. Goulding, Phys. Rev. Lett. **44**, 1751 (1980).

[5] C. D. Goodman, C. A. Goulding, M. B. Greenfield, J. Rapaport, D. E. Bainum, C. C. Foster, W. G. Love, and F. Petrovich, Phys. Rev. Lett. **44**, 1755 (1980).

[6] Carl Gaarde, Nucl. Phys. A **396**, 127 (1983).

[7] F. Osterfeld, Rev. Mod. Phys. **64**, 491 (1992).

[8] M. Ichimura, H. Sakai, and T. Wakasa, Prog. Part. Nucl. Phys. **56**, 446 (2006).

[9] A. B. Migdal, Rev. Mod. Phys. **50**, 107 (1978).

[10] K. Langanke and G. Martínez-Pinedo, Rev. Mod. Phys. **75**, 819 (2003).

[11] H. V. Klapdor-Kleingrothaus, *60 Years of Double Beta Decay : From Nuclear Physics to Beyond Standard Model Particle Physics* (World Scientific, Singapore, 2001).

[12] A. Akmal and V. R. Pandharipande, Phys. Rev. C **56**,

2261 (1997).

[13] J. Meyer-Ter-Vehn, Phys. Rep. **74**, 323 (1981).

[14] T. Wakasa *et al.*, Phys. Rev. C **85**, 064606 (2012).

[15] T. Suzuki, Nucl. Phys. A **379**, 110 (1982).

[16] T. Wakasa, M. Ichimura, and H. Sakai, Phys. Rev. C **72**, 067303 (2005).

[17] Y. F. Niu, G. Colò, M. Brenna, P. F. Bortignon, and J. Meng, Phys. Rev. C **85**, 034314 (2012).

[18] T. N. Taddeucci, C. A. Goulding, T. A. Carey, R. C. Byrd, C. D. Goodman, C. Gaarde, J. Larsen, D. Horen, J. Rapaport, and E. Sugarbaker, Nucl. Phys. A **469**, 125 (1987).

[19] M. Sasano *et al.*, Phys. Rev. Lett. **107**, 202501 (2011).

[20] M. Sasano *et al.*, Phys. Rev. C **86**, 034324 (2012).

[21] T. Kobayashi *et al.*, Nucl. Instrum. Methods Phys. Res. B **317**, 294 (2013).

[22] K. Yako *et al.*, RIKEN Accel. Prog. Rep. **45**, 137 (2012).

[23] J. Yasuda *et al.*, Nucl. Instrum. Methods Phys. Res. B **376**, 393 (2016).

[24] S. Agostinelli *et al.*, Nucl. Instrum. Methods Phys. Res. A **506**, 250 (2003).

[25] K. Kawahigashi, K. Nishida, A. Itabashi, and M. Ichimura, Phys. Rev. C **63**, 044609 (2001).

[26] M. A. Franey and W. G. Love, Phys. Rev. C **31**, 488 (1985).

[27] S. Hama, B. C. Clark, E. D. Cooper, H. S. Sherif, and R. L. Mercer, Phys. Rev. C **41**, 2737 (1990).

[28] E. D. Cooper, S. Hama, B. C. Clark, and R. L. Mercer, Phys. Rev. C **47**, 297 (1993).

[29] S. Qing-biao, F. Da-chun, and Z. Yi-zhong, Phys. Rev. C **43**, 2773 (1991).

[30] M. Sasano *et al.*, Phys. Rev. C **79**, 024602 (2009).

[31] A. Bohr and B. R. Mottelson, *Nuclear Structure Volume I : Single-Particle Motion* (Benjamin, New York, 1969).

[32] K. Pham *et al.*, Phys. Rev. C **51**, 526 (1995).

[33] K. Nakayama, A. Pio Galeao, and F. Krmpotic, Phys. Lett. B **114**, 217 (1982).

[34] LAND-FRS Collaboration, P. Adrich *et al.*, Phys. Rev. Lett. **95**, 132501 (2005).

[35] O. Wieland *et al.*, Phys. Rev. Lett. **102**, 092502 (2009).

[36] G. Audi, O. Bersillon, J. Blachot, and A.H. Wapstra, Nucl. Phys. A **729**, 3 (2003).

[37] Y. F. Niu, G. Colò, and E. Vigezzi, Phys. Rev. C **90**, 054328 (2014).

[38] E. Litvinova, B.A. Brown, D.-L. Fang, T. Marketin, and R.G.T. Zegers, Physics Letters B **730**, 307 (2014).

[39] Haozhao Liang, Nguyen Van Giai, and Jie Meng, Phys. Rev. Lett. **101**, 122502 (2008).

[40] T. Marketin, E. Litvinova, D. Vretenar, and P. Ring, Physics Letters B **706**, 477 (2012).

[41] Haozhao Liang and Zhongming Niu, private communications.

[42] Z.-Y. Ma, B.-Q. Chen, N. Van Giai, and T. Suzuki, The European Physical Journal A - Hadrons and Nuclei **20**, 429 (2004).

[43] C. Robin and E. Litvinova, Relativistic approach to nuclear spin-isospin excitations including quasiparticle-vibration coupling, in *Proceedings of Science (INPC2016)* Vol. 281, p. 020, 2017.

[44] Y. F. Niu and G. Colò, private communications.

[45] E. Litvinova, C. Robin, Y. F. Niu, G. Colò, H. Liang, and Z. Niu, private communications.